REPORTS

COMETARY SCIENCE

Seasonal exposure of carbon dioxide ice on the nucleus of comet 67P/Churyumov-Gerasimenko

G. Filacchione,[1]* A. Raponi,[1] F. Capaccioni,[1] M. Ciarniello,[1] F. Tosi,[1] M. T. Capria,[1] M. C. De Sanctis,[1] A. Migliorini,[1] G. Piccioni,[1] P. Cerroni,[1] M. A. Barucci,[2] S. Fornasier,[2] B. Schmitt,[3] E. Quirico,[3] S. Erard,[2] D. Bockelee-Morvan,[2] C. Leyrat,[2] G. Arnold,[4] V. Mennella,[5] E. Ammannito,[6] G. Bellucci,[1] J. Benkhoff,[7] J. P. Bibring,[8] A. Blanco,[9] M. I. Blecka,[10] R. Carlson,[11] U. Carsenty,[3] L. Colangeli,[7] M. Combes,[2] M. Combi,[12] J. Crovisier,[2] P. Drossart,[2] T. Encrenaz,[2] C. Federico,[13] U. Fink,[14] S. Fonti,[9] M. Fulchignoni,[2] W.-H. Ip,[15] P. Irwin,[16] R. Jaumann,[4] E. Kuehrt,[4] Y. Langevin,[8] G. Magni,[1] T. McCord,[17] L. Moroz,[4] S. Mottola,[4] E. Palomba,[1] U. Schade,[18] K. Stephan,[4] F. Taylor,[16] D. Tiphene,[2] G. P. Tozzi,[19] P. Beck,[3] N. Biver,[2] L. Bonal,[3] J.-Ph. Combe,[17] D. Despan,[2] E. Flamini,[20] M. Formisano,[1] A. Frigeri,[1] D. Grassi,[1] M. S. Gudipati,[11] D. Kappel,[4] A. Longobardo,[1] F. Mancarella,[9] K. Markus,[4] F. Merlin,[2] R. Orosei,[21] G. Rinaldi,[1] M. Cartacci,[1] A. Cicchetti,[1] Y. Hello,[2] F. Henry,[2] S. Jacquinod,[2] J. M. Reess,[2] R. Noschese,[1] R. Politi,[1] G. Peter[22]

Carbon dioxide (CO_2) is one of the most abundant species in cometary nuclei, but because of its high volatility, CO_2 ice is generally only found beneath the surface. We report the infrared spectroscopic identification of a CO_2 ice–rich surface area located in the Anhur region of comet 67P/Churyumov-Gerasimenko. Spectral modeling shows that about 0.1% of the 80- by 60-meter area is CO_2 ice. This exposed ice was observed a short time after the comet exited local winter; following the increased illumination, the CO_2 ice completely disappeared over about 3 weeks. We estimate the mass of the sublimated CO_2 ice and the depth of the eroded surface layer. We interpret the presence of CO_2 ice as the result of the extreme seasonal changes induced by the rotation and orbit of the comet.

On comets, sublimation caused by solar illumination is the major mechanism that differentiates volatile species over their long dynamical lifetimes. The penetration of heat into the comet's nucleus causes chemical stratification, with more volatile molecules, such as CO and CO_2, receding into the interior ices, whereas less volatile molecules, such as water, remain close to the surface and enrich the near-surface ices (*1*). The seasonal variability associated with the relatively large orbital eccentricities of comets is further complicated by the irregular shape of their nuclei and the inclination of their rotational axes, which amplify the seasonal effects. Thus far, thermal evolution models have not provided evidence of recondensation or fast sublimation of volatile species following an extreme seasonal cycle. Evidence from the comet 67P/Churyumov-Gerasimenko (67P/CG) confirmed the general volatiles stratification scheme during the preperihelion period, when the spatial distribution of water vapor and CO_2 in the gaseous coma was interpreted as the result of CO_2 ice sublimating from inner layers, with water ice sublimating closer to the surface (*2*–*6*). A diurnal cycle of water ice has been observed in which an ephemeral frost layer forms in response to sudden shadowing conditions and day-night variation (*7*).

In early 2015, the southern hemisphere of 67P/CG was emerging from shadows and leaving its cold season, during which subsurface temperatures were as low as 25 to 50 K (*8*). In particular, an area located in the Anhur region [at longitude 66.06° and latitude −54.56° in Cheops coordinate frame (*9*)] had experienced a 4-year-long winter season before being illuminated by the Sun in mid-January 2015.

Using the VIRTIS-M (Visible, Infrared and Thermal Imaging Spectrometer, Mapping Channel) onboard the Rosetta spacecraft (*10*), we detected a CO_2 ice–rich area in the Anhur region on 21–22 March 2015, when the comet was 2.05 astronomical units (AU) from the Sun. This region is 80 by 60 m (resolved at 20 m per pixel in VIRTIS-M images) and is shown in the general context of the nucleus digital shape model in Fig. 1. The deposit is located in a smooth area of the Anhur region, on the large lobe of the nucleus (*11*). The same spectral data set, for which we give additional details in (*12*), has been used to derive quantitative information on CO_2 abundance. The irradiance/solar flux (I/F) spectrum of the pixel with the most intense absorption features is shown in Fig. 2. The I/F spectrum is characterized by a steep red spectral slope up to 1.5 μm; an absorption triplet at 1.97, 2.01, and 2.07 μm; and two further absorptions at 2.7 and 2.78 μm. These features correspond to known absorption features of CO_2 and thus indicate the presence of CO_2 ice on the surface of 67P/CG. The CO_2 ice fundamental band at 4.26 μm is not visible in the I/F spectra because of the thermal emission from the nucleus. Detailed descriptions of the spectral variability across the CO_2 ice–rich area, the removal of the thermal emission signal, and the spectral modeling are given in (*12*).

The spectra of the CO_2 ice–rich area have been fitted with a radiative transfer model (*13*, *14*), allowing us to derive quantitative information on end-member abundances, mixing modalities, and grain sizes. The I/F spectrum is simulated by using areal and intimate mixtures of two components: the dark terrain (DT) unit, corresponding to the measured average organic-rich spectrum of the comet's surface (*15*) after the application of photometric correction (*16*), and CO_2 ice derived from optical constants (*17*, *18*). The composition of the DT unit, characterized by low albedo, a red slope, and a broad absorption feature in the 3.2-μm range, is still uncertain (*19*). To check the quality of the spectral retrieval, we performed an additional fit by replacing CO_2 ice with crystalline water ice (*20*–*22*). The VIRTIS spectral mixing and data processing methods are described at length in previous works (*23*, *24*). The modeling of each individual pixel in which CO_2 ice was detected is discussed in (*12*).

The results of the spectral modeling are shown in the left panel of Fig. 2. The best-fitting model including a water ice component requires 99.7% DT with a slope (necessary to correct for photometric response) of −3.8% μm^{-1}, plus 32-μm water ice grains in areal mixing for the remaining 0.3%. The quality of this fit is very poor, however ($\chi^2 = 3.85$), in particular in the 2.0-μm and 2.7- to 2.8-μm ranges, where water ice is

[1]INAF-IAPS (Istituto Nazionale di AstroFisica–Istituto di Astrofisica e Planetologia Spaziali), Rome, Italy. [2]Laboratoire d'Études Spatiales et d'Instrumentation en Astrophysique, Observatoire de Paris, Paris Sciences and Letters Research University, CNRS (Centre National de la Recherche Scientifique), Sorbonne Universités, UPMC (Université Pierre et Marie Curie) Université Paris 06, Université Paris Diderot, Sorbonne Paris Cité, France. [3]Université Grenoble Alpes, CNRS, Institut de Planetologie et d'Astrophysique de Grenoble, Grenoble, France. [4]Institute for Planetary Research, DLR (Deutschen Zentrums für Luft- und Raumfahrt), Berlin, Germany. [5]INAF Osservatorio di Capodimonte, Naples, Italy. [6]Department of Earth, Planetary, and Space Sciences, University of California–Los Angeles, 603 Charles Young Drive, Los Angeles, CA 90095-1567, USA [7]ESA (European Space Agency), European Space Research and Technology Centre, Noordwijk, Netherlands. [8]Institut d'Astrophysique Spatial, CNRS, Orsay, France. [9]Dipartimento di Matematica e Fisica "Ennio De Giorgi," Università del Salento, Lecce, Italy. [10]Space Research Centre, Polish Academy of Sciences, Warsaw, Poland. [11]NASA JPL (Jet Propulsion Laboratory), California Institute of Technology, Pasadena, CA 91109, USA. [12]Space Physics Research Laboratory, The University of Michigan, Ann Arbor, MI 48109, USA. [13]Università di Perugia, Perugia, Italy. [14]Lunar Planetary Laboratory, University of Arizona, Tucson, AZ 85721, USA. [15]National Central University, Taipei, Taiwan. [16]Departement of Physics, Oxford University, Oxford, UK. [17]Bear Fight Institute, Winthrop, WA 98862, USA. [18]Helmholtz-Zentrum Berlin für Materialien und Energie, Berlin, Germany. [19]INAF Osservatorio Astrofisico di Arcetri, Firenze, Italy. [20]Agenzia Spaziale Italiana, Rome, Italy. [21]INAF Istituto di Radioastronomia, Bologna, Italy. [22]Institute of Optical Sensor Systems, DLR, Berlin, Germany.
*Corresponding author. Email: gianrico.filacchione@iaps.inaf.it

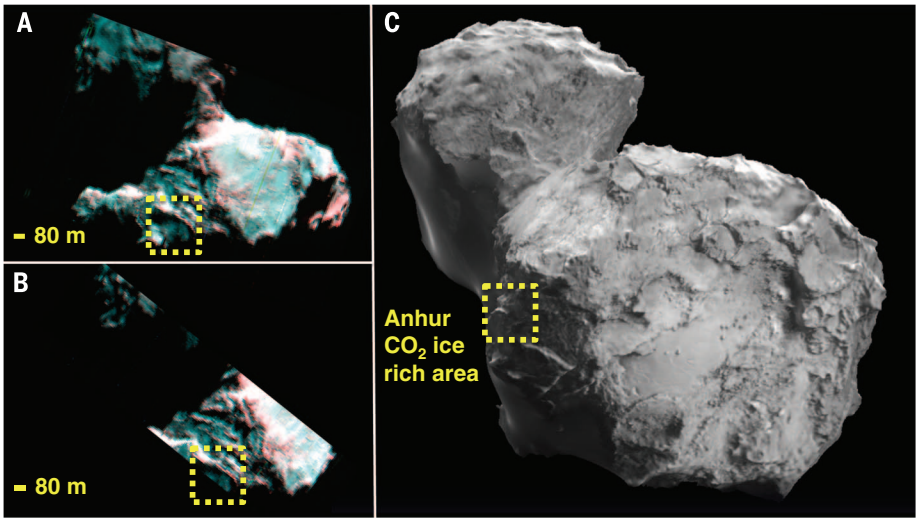

Fig. 1. VIRTIS-M infrared images of the Anhur CO_2 ice–rich area, 21–22 March 2015. The center of the yellow dashed box is the location of the CO_2-rich patch in VIRTIS-M images (**A**) I1_00385598211 and (**B**) I1_00385688463, as well as (**C**) on the nucleus shape model (from http://sci.esa.int/comet-viewer/?model=esa). VIRTIS-M color images are a RGB combination of infrared bands (blue at 1.2 μm, green at 2.0 μm, and red at 4.0 μm). A description of the VIRTIS-M acquisitions is given in (*12*).

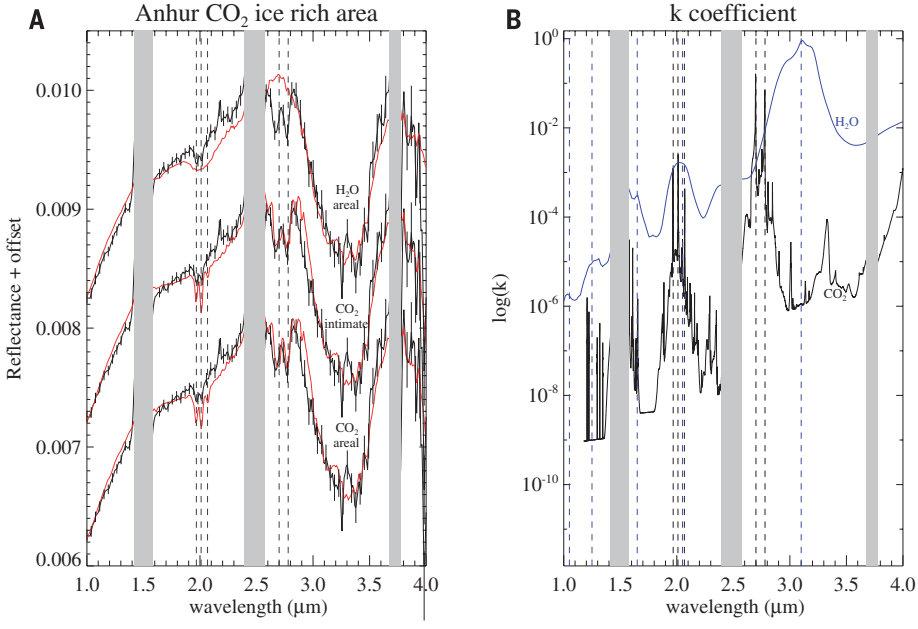

Fig. 2. Spectral modeling of the CO_2 surface ice from the 21 March 2015 observation. (**A**) VIRTIS-M reflectance (black curve, from observation I1_00385598211; pixel s = 126, l = 109) and spectral simulations carried out with dark terrain (DT) and H_2O ice in areal mixing (top, plus 0.002 offset), DT and CO_2 ice in intimate mixing (center, plus 0.001 offset), and DT and CO_2 ice in areal mixing (bottom) for the Anhur CO_2 ice–rich area. Spectral intervals shaded in gray correspond to data that are missing as a result of instrumental order sorting filters. Error bars, shown every five bands to improve readability, give the instrument noise on the pixel. (**B**) Imaginary part k of refractive indices for H_2O ice (blue curve) and CO_2 ice (black curve). Optical constants for CO_2 are from (*17*, *18*) and for H_2O are from (*20*–*22*). Vertical lines mark the k local maxima corresponding to the strongest absorption bands at 1.05, 1.25, 1.65, 2.05, and 3.10 μm for H_2O ice (in blue) and at 1.97, 2.01, 2.07, 2.70, and 2.78 μm for CO_2 ice [in black; also shown in (A)].

not able to reproduce the observed absorption features, indicating its absence in this area. Better fits are achieved by replacing water with CO_2 ice (Fig. 2). We show two possible models. The first corresponds to an intimate mixing (*12*) of 99.2% DT with a –5.12% μm^{-1} slope, plus 0.8% 800-μm CO_2 ice grains. The second case corresponds to an areal mixing of 99.9% DT with a slope of –4.76% μm^{-1}, plus 0.1% 50-μm CO_2 ice grains. With a residual of χ^2 = 2.05, the areal solution appears marginally better than the intimate, for which χ^2 = 2.45. The addition of water ice to the components of the mixture does not improve the fit quality. In both models, less than 1% CO_2 ice is sufficient to account for the observed spectral absorption features.

The CO_2 ice features were detected on 2 consecutive days (21 and 22 March 2015). This means that the CO_2 ice area was stable against day-night variations in temperature. However, after the March detection, VIRTIS-M did not observe the Anhur region again until 12–13 April 2015, when the heliocentric distance was reduced to 1.87 AU and the pixel scale was reduced from 20 to 39 m per pixel. At this time, the spectra acquired did not show any of the previously observed CO_2 absorption features (Fig. 3), indicating that the CO_2 ice patch had diminished to a level below the detection limit of the VIRTIS-M instrument (band depth less than 1% relative to the local continuum, corresponding to <0.1% CO_2 ice abundance), if not disappeared altogether. The reduction of the spatial resolution by a factor of about 2 and the increase of the solar phase angle from 54° to 79° between the two sets of observations must be considered in interpreting the disappearance of the CO_2 ice spectral features: Apart from the change in spatial resolution, the last images are more affected by long shadows caused by local topography, making the detection of the CO_2 ice more difficult. Conversely, assuming a uniform distribution of CO_2 ice in areal mixing with the DT within the initial 80- by 60-m area, one should expect to also detect it on the less resolved images because the instrumental resolution is still within the size of the area of interest.

The maximum surface temperature, derived by modeling the thermal emission at 4.5 to 5.0 μm with a Bayesian method (*25*), increased in this area from 218.8 K on 21 March 2015 to 225.9 K on 13 April 2015. However, given that the surface is not isothermal at the subpixel scale because of local roughness and shadows, these should be considered as upper limits, representative only of the warmest fractions of the pixel, corresponding to the more illuminated subpixel areas. The measured temperatures are well above the sublimation temperature of CO_2 ice, which is about 80 K (*26*); therefore, the CO_2 ice–rich region cannot be in thermal equilibrium with the DT, and continuous sublimation must occur. For this reason, intimate mixing between CO_2 ice and DT is much less favorable than areal mixing. As a result of the sublimation of the volatile species on the surface, an increase in the local roughness of the more illuminated areas is very likely to occur.

We investigated the illumination history of the Anhur CO_2 ice–rich area by tracing the variation of the incident solar flux during the time for which VIRTIS-M observations are available. Throughout the period from January 2011 to January 2015, the Anhur region was in permanent shadow, whereas from 14 January 2015 forward, the combined effect of decreasing heliocentric distance and longer insolation caused a net increase of solar flux to the area (Fig. 4). After scaling the instantaneous solar flux with the cosine of the incidence angle calculated using the nucleus

digital shape model (*27*, *28*), we found that at the time of the CO_2 ice detection (21–22 March 2015), the maximum solar flux at local noon was about 80 W/m^2 (Fig. 4). At the time of the second series of VIRTIS-M observations, the maximum solar flux at local noon had increased to about 135 W/m^2.

The integrated solar flux accumulated by an area of 0.4 m^2, corresponding to the CO_2 areal occupancy within the 400-m^2 VIRTIS-M pixel, is equal to 2.026×10^7 J over the 45 rotations of the comet occurring between the available VIRTIS-M observations. Assuming a latent heat of sublimation of 552 kJ/kg for CO_2 ice (*26*) and neglecting the thermal conduction in view of the very low thermal inertia reported for 67P/CG (*8*, *29*), we derive a value for the total amount of sublimated ice of 35 kg, equivalent to the erosion of a 5.6-cm-thick layer [further details are given in (*12*)]. This value is an upper limit, assuming a complete sublimation of the ice during 45 rotations. A similar estimate, performed from the beginning of the illumination conditions in early January 2015 until the time of the CO_2 ice detection, gives an additional sublimated ice mass of 22 kg. Hence, the area within a VIRTIS-M pixel experienced a maximum sublimation of 57 kg of CO_2 ice, corresponding to the erosion of a 9-cm layer, in about 3 months. The temporal trend of the cumulative CO_2 ice sublimation mass is shown in Fig. 4.

This amount of sublimated CO_2 ice is too small to contribute meaningfully to the gaseous coma emissions. Above the southern hemisphere, VIRTIS has detected a CO_2/H_2O ratio of about 4% (*4*), but no evidence has been found in VIRTIS-M spectra of increased H_2O or CO_2 gaseous activity in the surroundings of the Anhur region. In fact, even assuming a sublimation rate of 1 kg of CO_2 ice per day from a 20- by 20-m area, the resulting column density of 10^{17} m^{-2} in the ambient coma is about two orders of magnitude lower than the average value of 10^{19} m^{-2} measured by VIRTIS-M (*4*).

The observation of the CO_2 ice–rich spot was unexpected at these heliocentric distances, given the high volatility of CO_2; water ice, a less volatile species, was not observed in the same region at the same time, as confirmed by the spectral fit shown in fig. S5 (*12*). 67P/CG falls in the ensemble of the CO_2-rich comets, as demonstrated by the high activity level of CO_2 above the southern hemisphere, where the CO_2/H_2O ratio is considerably larger than in the northern hemisphere (*4*, *30*).

The OSIRIS (Optical, Spectroscopic, and Infrared Remote Imaging System) instrument did observe water ice in this same region (*31*) in April–May 2015, about 6 weeks after the initial detection of the CO_2 ice by VIRTIS-M. At this time (by 4 May 2015), the VIRTIS-M infrared channel had stopped operating because of the permanent failure of the active cooler, making it impossible to further study the temporal evolution of the Anhur region. Until then, the entire part of the southern hemisphere illuminated by the Sun was observed by VIRTIS-M with a spatial resolution between 20 and 40 m per pixel. So far, CO_2 ice has been recognized only in the Anhur region discussed in this study, localized approximately

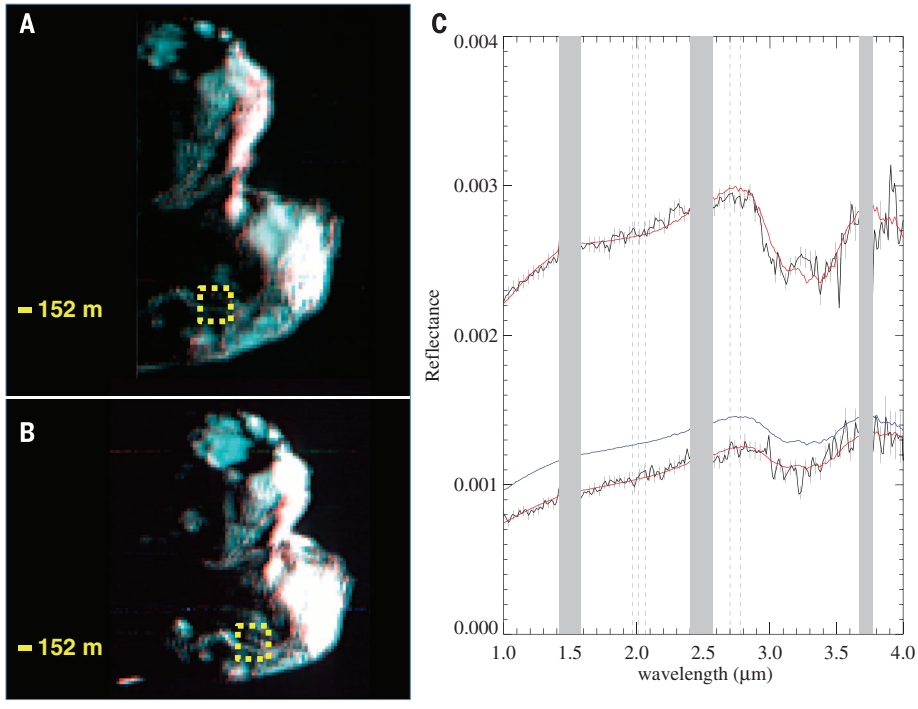

Fig. 3. The disappearance of the CO_2 surface ice by 12–13 April 2015. VIRTIS-M acquisitions (**A**) I1_00387470597 and (**B**) I1_00387561494. The position of the previously observed Anhur CO_2 ice deposit is at the center of the yellow dashed box in each panel. (**C**) Reflectance data from the boxed areas in the two acquisitions [bottom (A) and top (B) black lines] do not show the diagnostic triplet absorption at 2.0 μm or the bands at 2.7 and 2.78 μm (dashed vertical lines). The wide feature at 3.2 μm is the DT absorption due to organic material, the depth of which is correlated with the local reflectance level. Spectral modeling results with pure DT are shown in red. For reference, the average DT reflectance derived from (*16*) is shown in blue. A description of the spectral modeling is given in (*12*).

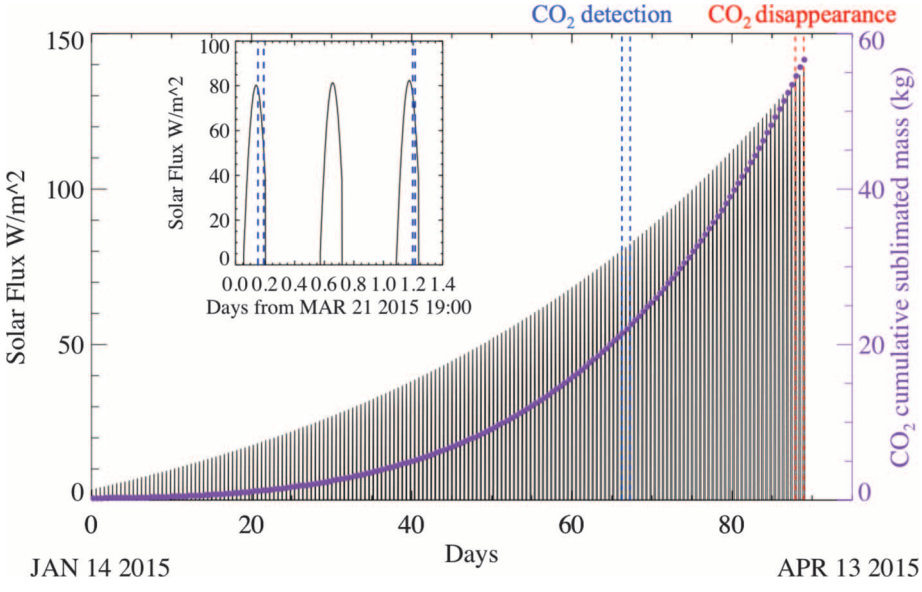

Fig. 4. Variation of solar flux reaching the Anhur CO_2 ice–rich area between 14 January and 13 April 2015. The vertical dashed lines indicate the timing of the four VIRTIS observations described in the text: CO_2 ice was detected during the first two (marked in blue; a close-up view is shown in the inset), whereas it had disappeared by the time of the last two (marked in red). The cumulative mass of sublimated CO_2 during this time frame is shown by the purple curve. All values are relative to one VIRTIS pixel area (20 by 20 m) at the time of CO_2 detection.

between a slope and a flat terrain showing a regular topography in OSIRIS images (*31*). The morphology and illumination conditions at this place are similar to those of many nearby areas observed by VIRTIS-M.

The presence of CO_2 ice at the surface of the nucleus thus appears to be an ephemeral occurrence, which provides clues to the emplacement mechanism. After perihelion passage, the activity of a cometary nucleus starts to decrease, with water sublimation decreasing first. Nucleus thermodynamical modeling (*1*) shows that a stratigraphy associated to the volatility of the major gaseous species is produced in the outer layers of 67P/CG. However, the combination of spin axis inclination and nucleus shape means that the Anhur CO_2 ice–rich area experiences a fast drop in illumination, going into permanent shadow quickly after equinox and, consequently, undergoing a rapid reduction in surface temperatures in winter to less than 80 K, whereas the interior remains warmer for a longer time because of the low thermal inertia (*8*, *29*). Sublimation of water ice at depth is prevented, but sublimation of CO_2 ice is not; CO_2 can continue to flow from the interior to the surface, where it begins to freeze as a result of the low surface temperatures. Moving further toward the aphelion, the low surface temperatures preserve the CO_2 ice on the surface, which grows in >100-μm grains until, on the next orbit, it is exposed again to sunlight and sublimates away. This inverse temperature profile of cometary surfaces (warmer inside and cooler on the surface) going into winter after perihelion (in permanently shadowed regions) could potentially freeze other volatiles that are sublimed from the warmer interior as well. Based on the temperature of these surface areas, more volatiles species such as CO and CH_4 could also be frozen until the next exposure to solar photons occurs. The same phenomenon could also explain why no water ice was seen at this site during the initial exposure to the Sun, because the water ice would have been frozen at lower depths than the CO_2 ice.

The 67P/CG nucleus shows two different temporal activity cycles respectively caused by H_2O and CO_2 ices in different regions: Whereas water ice has diurnal variability, with a surface sublimation and condensation cycle occurring in the most active areas (*7*), the surface condensation of CO_2 ice has a seasonal dependence. Similar processes are probably common among many Jupiter-family comets, which share with 67P/CG short revolution periods and eccentric orbits (*32*).

REFERENCES AND NOTES

1. M. C. De Sanctis, M. T. Capria, A. Coradini, *Adv. Space Res.* **38**, 1906–1910 (2006).
2. M. Hässig *et al.*, *Science* **347**, aaa0276 (2015).
3. D. Bockelée-Morvan *et al.*, *Astron. Astrophys.* **583**, A6 (2015).
4. A. Migliorini *et al.*, *Astron. Astrophys.* **589**, A45 (2016).
5. N. Fougere *et al.*, *Astron. Astrophys.* **588**, A134 (2016).
6. U. Fink *et al.*, *Icarus* **277**, 78–97 (2016).
7. M. C. De Sanctis *et al.*, *Nature* **525**, 500–503 (2015).
8. M. Choukroun *et al.*, *Astron. Astrophys.* **583**, A28 (2015).
9. F. Preusker *et al.*, *Astron. Astrophys.* **583**, A33 (2015).
10. A. Coradini *et al.*, *Space Sci. Rev.* **128**, 529–559 (2007).
11. M. R. El-Maarry *et al.*, *Astron. Astrophys.* **593**, A110 (2016).
12. Materials and methods are available as supplementary materials on *Science* Online.
13. B. Hapke, *Theory of Reflectance and Emittance Spectroscopy* (Cambridge Univ. Press, 2012).
14. M. Ciarniello *et al.*, *Icarus* **214**, 541–555 (2011).
15. F. Capaccioni *et al.*, *Science* **347**, aaa0628 (2015).
16. M. Ciarniello *et al.*, *Astron. Astrophys.* **583**, A31 (2015).
17. E. Quirico, B. Schmitt, *Icarus* **127**, 354–378 (1997).
18. E. Quirico *et al.*, *Icarus* **139**, 159–178 (1999).
19. E. Quirico *et al.*, *Icarus* **272**, 32–47 (2016).
20. S. G. Warren, *Appl. Opt.* **23**, 1206 (1984).
21. R. M. Mastrapa, S. A. Sandford, T. L. Roush, D. P. Cruikshank, C. M. Dalle Ore, *Astrophys. J.* **701**, 1347–1356 (2009).
22. R. N. Clark *et al.*, *Icarus* **218**, 831–860 (2012).
23. G. Filacchione *et al.*, *Nature* **529**, 368–372 (2016a).
24. G. Filacchione *et al.*, *Icarus* **274**, 334–349 (2016b).
25. F. Tosi *et al.*, *Icarus* **240**, 36–57 (2014).
26. W. F. Huebner, J. Benkhoff, M-T. Capria, A. Coradini, C. De Sanctis, R. Orosei, D. Prialnik, "Heat and gas diffusion in comet nuclei" (International Space Science Institute report SR-004, ESA Publications Division, 2006).
27. L. Jorda, R. H. Gaskell, Shape models of 67P/Churyumov-Gerasimenko, RO-C-OSINAC/OSIWAC-5-67P-SHAPE-V1.0 (NASA Planetary Data System and ESA Planetary Science Archive, 2015); https://pds.nasa.gov/ds-view/pds/viewProfile.jsp?dsid=RO-C-OSINAC/OSIWAC-5-67P-SHAPE-V1.0.
28. L. Jorda *et al.*, *Icarus* **277**, 257–278 (2016).
29. F. P. Schloerb *et al.*, *Astron. Astrophys.* **583**, A29 (2015).
30. D. Bockelée-Morvan *et al.*, *Mon. Not. R. Astron. Soc.* 10.1093/mnras/stw2428 (2016).
31. S. Fornasier *et al.*, *Science* **354**, 1566–1570 (2016).
32. D. Jewitt, *Earth Moon Planets* **79**, 35–53 (1997).

ACKNOWLEDGMENTS

The authors thank the institutions and agencies that supported this work: the Italian Space Agency (ASI), Centre National d'Etudes Spatiales (CNES, France), DLR (Germany), and NASA (USA). VIRTIS was built by a consortium from Italy, France, and Germany, under the scientific responsibility of INAF-IAPS, Rome, Italy, which also led the scientific operations. The VIRTIS instrument development for ESA has been funded and managed by ASI, with contributions from Observatoire de Meudon (financed by CNES) and DLR. The VIRTIS instrument industrial prime contractor was formerly Officine Galileo and is now Leonardo SpA in Campi Bisenzio, Florence, Italy. The authors thank the Rosetta Liaison Scientists, the Rosetta Science Ground Segment, and the Rosetta Mission Operations Centre for their support in planning the VIRTIS observations. T.M. acknowledges additional funding from NASA JPL, W.-H.I. from the National Science Council of Taiwan (grant 102-2112-M-008-013-MY3) and Science and Technology Development Fund of Macao Special Administrative Region (grant 017/2014/A1), and L.M. from Deutsche Forschungsgemeinschaft (grant MO 3007/1-1). The VIRTIS calibrated data are available through ESA's Planetary Science Archive (www.cosmos.esa.int/web/psa/rosetta). This research has made use of NASA's Astrophysics Data System.

SUPPLEMENTARY MATERIALS

www.sciencemag.org/content/354/6319/1563/suppl/DC1
Materials and Methods
Figs. S1 to S8
Table S1
References (*33*–*41*)

8 June 2016; accepted 28 October 2016
Published online 17 November 2016
10.1126/science.aag3161

COMETARY SCIENCE

Rosetta's comet 67P/Churyumov-Gerasimenko sheds its dusty mantle to reveal its icy nature

S. Fornasier,[1]* S. Mottola,[2] H. U. Keller,[2,3] M. A. Barucci,[1] B. Davidsson,[4] C. Feller,[1] J. D. P. Deshapriya,[1] H. Sierks,[5] C. Barbieri,[6] P. L. Lamy,[7] R. Rodrigo,[8,9] D. Koschny,[10] H. Rickman,[11,12] M. A'Hearn,[13] J. Agarwal,[5] J.-L. Bertaux,[14] I. Bertini,[6] S. Besse,[15] G. Cremonese,[16] V. Da Deppo,[17] S. Debei,[18] M. De Cecco,[19] J. Deller,[5] M. R. El-Maarry,[20] M. Fulle,[21] O. Groussin,[22] P. J. Gutierrez,[8] C. Güttler,[5] M. Hofmann,[5] S. F. Hviid,[2] W.-H. Ip,[23,24] L. Jorda,[22] J. Knollenberg,[2] G. Kovacs,[5,25] R. Kramm,[5] E. Kührt,[2] M. Küppers,[15] M. L. Lara,[8] M. Lazzarin,[6] J. J. Lopez Moreno,[8] F. Marzari,[6] M. Massironi,[26,27] G. Naletto,[28,27,17] N. Oklay,[5] M. Pajola,[29,27] A. Pommerol,[20] F. Preusker,[2] F. Scholten,[2] X. Shi,[5] N. Thomas,[20] I. Toth,[30] C. Tubiana,[5] J.-B. Vincent[5]

The Rosetta spacecraft has investigated comet 67P/Churyumov-Gerasimenko from large heliocentric distances to its perihelion passage and beyond. We trace the seasonal and diurnal evolution of the colors of the 67P nucleus, finding changes driven by sublimation and recondensation of water ice. The whole nucleus became relatively bluer near perihelion, as increasing activity removed the surface dust, implying that water ice is widespread underneath the surface. We identified large (1500 square meters) ice-rich patches appearing and then vanishing in about 10 days, indicating small-scale heterogeneities on the nucleus. Thin frosts sublimating in a few minutes are observed close to receding shadows, and rapid variations in color are seen on extended areas close to the terminator. These cyclic processes are widespread and lead to continuously, slightly varying surface properties.

All cometary nuclei observed to date have appeared to be dark, with only a limited amount of water ice detected in small patches (*1*, *2*), although water is the dominant volatile observed in their coma.

The Rosetta spacecraft has been orbiting comet 67P/Churyumov-Gerasimenko since August 2014, providing the opportunity to continuously investigate its nucleus. The comet has a distinct bilobate shape and a complex morphology (*3*–*5*), with a

Science

Seasonal exposure of carbon dioxide ice on the nucleus of comet 67P/Churyumov-Gerasimenko

G. FilacchioneA. RaponiF. CapaccioniM. CiarnielloF. TosiM. T. CapriaM. C. De SanctisA. MiglioriniG. PiccioniP. CerroniM. A. BaruccS. FornasierB. SchmittE. QuiricoS. ErardD. Bockelee-MorvanC. LeyratG. ArnoldV. MennellaE. AmmannitoG. BellucciJ. BenkhoffJ. P. BibringA. BlancoM. I. BleckaR. CarlsonU. CarsentyL. ColangeliM. CombesM. CombiJ. CrovisierP. DrossartT. EncrenazC. FedericoU. FinkS. FontiM. FulchignoniW.-H. IpP. IrwinR. JaumannE. KuehrtY. LangevinG. MagniT. McCordL. MorozS. MottolaE. PalombaU. SchadeK. StephanF. TaylorD. TipheneG. P. TozziP. BeckN. BiverL. BonalJ.-Ph. CombeD. DespanE. FlaminiM. FormisanoA. FrigeriD. GrassiM. S. GudipatiD. KappelA. LongobardoF. MancarellaK. MarkusF. MerlinR. OroseiG. RinaldiM. CartacciA. CicchettiY. HelloF. HenryS. JacquinodJ. M. ReessR. NoscheseR. PolitiG. Peter

Science, 354 (6319), • DOI: 10.1126/science.aag3161

Rosetta observes sublimating surface ices

Comets are “dirty snowballs” made of ice and dust, but they are dark because the ice sublimates away, leaving some of the dust behind on the surface. The Rosetta spacecraft has provided a close-up view of the comet 67P/Churyumov-Gerasimenko as it passes through its closest point to the Sun (see the Perspective by Dello Russo). Filacchione *et al.* detected the spectral signature of solid CO (dry ice) in small patches on the surface of the nucleus as they emerged from local winter. By modeling how the CO sublimates, they constrain the composition of comets and how ices generate the gaseous coma and tail. Fornasier *et al.* studied images of the comet and discovered bright patches on the surface where ice was exposed, which disappeared as the ice sublimated. They also saw frost emerging from receding shadows. The surface of the comet was noticeably less red just after local dawn, indicating that icy material is removed by sunlight during the local day.

Science, this issue p. 1563, p. 1566; see also p. 1536

Science (ISSN 1095-9203) is published by the American Association for the Advancement of Science. 1200 New York Avenue NW, Washington, DC 20005. The title *Science* is a registered trademark of AAAS.